Rev. Roum. Sci. Techn.– Électrotechn. et Énerg.
Vol. 71, 3, pp. 457–462, Bucarest, 2026

Thermotechnique et thermoénergétique
Thermal engineering and thermal energy

COOLING LOAD IMPACT ON THE PERFORMANCE OF A PORTABLE THERMOELECTRIC REFRIGERATOR

GHULAM RAZA SHAH RIZVI[1], RAHOOL RAI[1], CLAUDIA SĂVESCU[2,3,*]

Keywords: Thermoelectric refrigerator; Peltier effect; Thermoelectric cooler (TEC); Heatsink performance; Cooling load impact.

This study investigates the influence of cooling load on the performance of a portable thermoelectric refrigerator based on the Peltier effect. A compact refrigeration system using a TEC1-12710 thermoelectric module powered at 12 V DC was experimentally analyzed under varying cooling loads, heatsink configurations, and convection modes. The system was divided into a refrigeration compartment and a hot-side heat dissipation area, where three different heatsinks were evaluated under natural and forced convection conditions. Experimental results demonstrate that the thermal characteristics and combination of cooling loads significantly affect the heat transfer rate, the cooling time and the coefficient of performance. Among the tested configurations, the optimized heatsink operating under forced convection achieved the highest heat transfer rate and coefficient of performance. Tests conducted with various food items and their combinations showed that increased thermal mass results in longer cooling times and higher energy demand. The findings highlight the importance of efficient heat dissipation and load management in improving the performance of portable thermoelectric refrigeration systems, particularly for low-power and mobile applications.

1. INTRODUCTION

Thermoelectric refrigeration has recently emerged as a viable alternative to traditional cooling methods, owing to its compactness, portability, environmental sustainability, and lack of moving parts [1–6]. The Peltier effect is fundamental to this technique, as electric current produces a temperature difference across a thermoelectric module. Conversely, the Seebeck effect is used by thermocouples and thermoelectric generators [7–12]. These modules are extensively used in portable refrigeration systems for purposes ranging from food preservation in household applications or medical transportation to industrial use, such as control cabinet cooling [13, 14]. The efficacy of such systems is considerably affected by the cooling load, referring to the quantity of thermal energy to be removed to sustain the desired temperature in the refrigerated area [2].

The cooling load directly influences the coefficient of performance (COP), a measure of a refrigerator's efficiency [15]. As cooling load increases, additional energy is needed to sustain a specified temperature, frequently leading to a reduction in COP. The decline in efficiency is more significant when cooling heavier items or many items concurrently. Additionally, external factors such as ambient temperature, convection type, and the configuration of heat exchangers and thermoelectric components can significantly influence the system's efficiency. Consequently, the interaction between cooling load and these factors is crucial for enhancing the system's overall efficiency [16, 17].

Chen et al. [1] studied the performance of a thermoelectric refrigerator under natural convection, aiming to obtain optimal heat rejection without fans by redesigning the TEC and increasing the dissipation area. The numerical and experimental results showed that the inside air temperature decreases as the fin height increases, but the cooling capacity and COP of the refrigerator exhibit little changes. Lv et al. [2] developed a multi-space portable thermoelectric studied a refrigerator with insulation, refrigeration, and freezing functions within three distinct compartments. The work optimizes module configuration and operating conditions to enhance energy efficiency through compartment temperature coupling, with tests performed on empty compartments. Afshari et al. [18] studied air-to-air thermoelectric refrigerators, cooling air inside a laboratory-scale cooling chamber, demonstrating that optimizing the geometry of the heat exchanger, by reducing its base thickness, significantly improves the cooling efficiency and cooling performance of the thermoelectric system. Abderezzak et al. [19] developed a novel thermoelectric refrigerator integrating finned heat pipes with enhanced heat sink technology. The experimental study was conducted exclusively using canned drinks as thermal load. The system demonstrated improved cooling performance compared to conventional thermoelectric refrigeration systems through its innovative heat sink design. Cüce et al. [20] investigated the use of nanofluids for hot-side cooling on a portable thermoelectric refrigerator in both loaded and unloaded test conditions. Lower cabinet temperatures and higher coefficients of performance were reported compared to water cooling. The study evaluates cabinet temperature, unloaded and loaded with 1 liter of water, cooling power, and COP for different nanoparticle concentrations. Alam et al. [21] developed a thermoelectric refrigerator using direct solar power and Peltier modules for off-grid applications. Testing an empty refrigerator compartment under outdoor conditions, the double module configuration with internal fans achieved optimal cooling performance, proving suitable for rural medicine storage.

Previous studies focused on investigating portable thermoelectric refrigerators and researching various cooling strategies. To our knowledge, no article systematically investigates the influence of different food products and their combined cooling loads on the thermal performance of portable thermoelectric refrigerators. Furthermore, a comparative evaluation under different heatsink configurations operating in both natural and forced convection conditions has not been reported.

The present study experimentally addresses this gap by

[1] Faculty of Engineering Science & Technology, Hamdard University, Karachi, 74600, Sindh, Pakistan.
[2] Romanian Research and Development Institute for Gas Turbines COMOTI, Bucharest, 061126, Romania.
[3] National University of Science and Technology Politehnica Bucharest, 060042, Romania.
E-mails: grizvitee19.ces@nust.edu.pk; rahool.rai@hamdard.edu; claudia.borzea@comoti.ro (corresponding author).

DOI: 10.59277/RRST-EE.2026.3.20

investigating the influence of different cooling loads on the performance of a portable thermoelectric refrigerator equipped with a TEC1-12710 module [22]. Different heatsink designs and convection modes are evaluated to determine the effects on heat transfer rate, cabinet temperature, and coefficient of performance (COP). The refrigerator is tested with individual food products as well as combinations of cooling loads, assessing the influence of thermal mass and load composition on cooling time, thermal performance, and energy efficiency.

The main contributions of this study are: (i) experimental evaluation of cooling load effects on COP and heat transfer rate in a portable thermoelectric refrigerator; (ii) comparative analysis of different heatsink designs under natural and forced convection; (iii) assessment of cooling performance for individual food items as well as for combined loads.

2. MATHEMATICAL MODEL AND DESIGN

The operating principle of the thermoelectric refrigerator is illustrated in Fig. 1. When a direct electric current passes through the thermoelectric (TE) module, heat is absorbed at the cold side and rejected at the hot side (Peltier effect). The thermal performance of the refrigerator is evaluated experimentally using temperature measurements, known load properties, and the electrical input power.

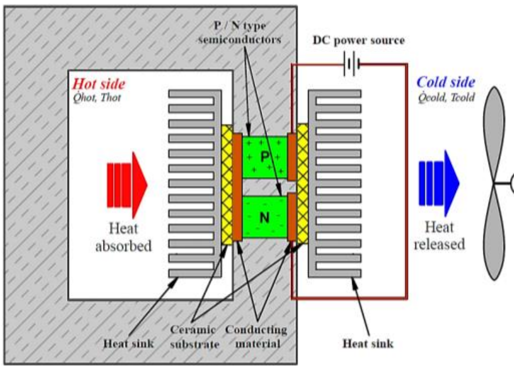

Fig. 1 – Peltier refrigeration schematic diagram.

The performance of a thermoelectric refrigerator depends on the accurate determination of temperature difference and cooling load. Two temperature differences are used and must be clearly distinguished, namely:

- **Module temperature difference** (across the TE module): ΔT_m, and the system (load) temperature change, ΔT_L, calculated as (1):

$$\Delta T_m = T_h - T_c \, , \tag{1}$$

where: ΔT_m [°C] – temperature difference across the thermoelectric module; T_h [°C] – hot side temperature; T_c [°C] – cold side temperature.

- **System (load) temperature change** (cooling of the refrigerated content) is defined as (2):

$$\Delta T_L = T_{L,0} - T_{L,f} \, , \tag{2}$$

where: ΔT_L [°C] – System temperature difference; $T_{L.0}$ [°C] – initial load temperature; $T_{L.f}$ [°C] – final load temperature.

For each tested specimen (or combination of specimens), the total heat removed from the load during a certain cooling interval is computed as (3):

$$Q_L = m c_P \Delta T_L \, , \tag{3}$$

where: Q_L [J] – total heat removed; m [kg] – load mass; c_p [J/(kg·K)] – specific heat capacity; ΔT_L [°C] – System temperature difference.

For the combinations of multiple refrigerated items, the heat removed is additive, being defined as (4):

$$Q_L = \sum_i m_i c_{p,i} \Delta T_L , \tag{4}$$

where: Q_L [J] – total heat removed; m_i [kg] – load item mass; $C_{p,i}$ [J/(kg·K)] – item specific heat capacity; $\sum m_i C_{p,i}$ [J/K] – Total heat capacity; ΔT_L [°C] – System temperature difference.

However, this is distinct from the system temperature difference, which is the temperature drop between the ambient and the load temperature.

The average cooling rate (average heat removal rate) has the expression in (5), which is consistent with the experimental procedure in which the time required for the load to reach a specified temperature drop is measured and used to compute $\dot{Q}_c$.

$$\dot{Q}_c = \frac{Q_L}{\Delta t} , \tag{5}$$

where: $\dot{Q}_c$ [W] – average cooling rate; Q_L [J] – total heat removed; Δt [s] – time interval.

The electrical power consumed by the refrigerator is defined as the system input power, being computed from measured voltage and current, (6):

$$P = VI , \tag{6}$$

where: P [W] – power; V [V] – voltage; I [A] – current.

Two power boundaries can be reported, namely:

- **System input power** (recommended for a practical refrigerator):

$$P_{in} = P_{TEC} + P_{fans} + P_{light} , \tag{7}$$

- **TEC-only input power** (for module comparison only):

$$P_{TEC} = V_{TEC} I_{TEC} \tag{8}$$

For consistency throughout the paper, the COP values were computed using the total system input power, including the TEC module, fans, and lighting, with an overall P_{in} for every test case.

The coefficient of performance (COP) for refrigeration, a key efficiency parameter, is:

$$COP_R = \frac{\dot{Q}_c}{P_{in}} , \tag{9}$$

where: COP_R [ND] – refrigeration coefficient of performance; $\dot{Q}_c$ [W] – average cooling rate at the cold side; P_{in} [W] – corresponding electrical input power, depending on the selected boundary.

This definition expresses the cooling power in watts per unit of electrical power input and is regarded as the standard definition of thermoelectric refrigeration performance.

The heat rejected at the hot side strongly depends on heatsink performance. For comparative evaluation of heatsinks, the effective thermal resistance can be computed using relation (10), relying on the measured temperatures and the heat flow through the heatsink:

$$R_{th} = \frac{T_b - T_a}{\dot{Q}_h}, \quad (10)$$

where: R_{th} [K/W] – heatsink thermal resistance near TE hot side; T_a [°C] – ambient air temperature; $\dot{Q}_h$ [W] – heat dissipated into ambient.

Assuming a sady operation, the hot side heat rate satisfies the following relation:

$$\dot{Q}_h \approx \dot{Q}_c + P_{TEC} \quad (11)$$

This relation provides a consistency check, as the rejected heat rate should exceed the cooling rate by approximately the electrical power supplied to the module (within measurement uncertainty and transient effects).

If the heat leak through the insulation is also considered, the conductive heat gain can be estimated using an overall thermal resistance, according to (12):

$$\dot{Q}_{leak} = \frac{T_a - T_{in}}{R_{ins}}, \quad (12)$$

with:

$$R_{ins} = \sum_i \frac{L_i}{k_i A_i}, \quad (13)$$

where: R_{ins} [K/W] – insulation thermal resistance; L_i [m] – insulation thickness; k_i [W/(m·K)] – thermal conductivity; A_i [m^2] – heat transfer area.

The critical insulation thickness under ideal cooling (ΔT = 40.4 °C) for a mass of 4.896 kg over 120 minutes was calculated with relation (14).

$$q = K\frac{\Delta T}{L} \Rightarrow L = \frac{K\Delta T}{q}, \quad (14)$$

A schematic representation of the insulation layers and the corresponding thermal resistances is illustrated in Fig. 2.

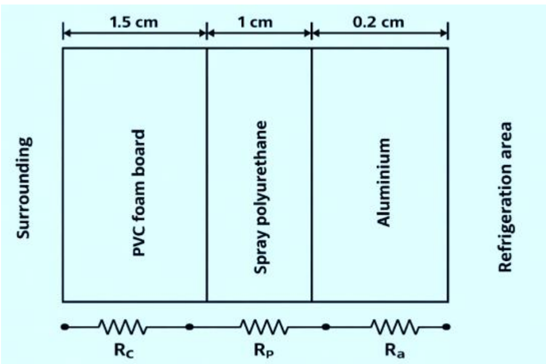

Fig. 2 – Schematic representation of the multilayer insulation system and equivalent thermal resistance network.

In each experimental test, the load temperature was monitored until achieving a fixed target temperature drop, ΔT_L. The required time, Δt, was recorded, and the average cooling rate, $\dot{Q}_c$, was computed using eq. (3)–(5). The refrigeration coefficient of performance was then calculated using expression (9) with the selected electrical power boundary (system power or TEC-only power, in our case the former). Heatsink performance comparisons are supported by considering the thermal resistance as defined in (10).

Table 1 summarizes the power requirements of the system components, calculated with relation (6). The power consumption of the fans, thermoelectric cooling module, and light source renders a total power demand of 108.6 W.

Table 1

Power Requirements of the System Components

Component	***V*** **[V]**	***I*** **[A]**	P_{unit} **[W]**	**Quantity**	***P*** **[W]**
Fan	12	0.40	4.8	3	14.4
Peltier Module	12	6.19	74.28	1	74.28
Light Source	12	1.66	19.92	1	19.92

The system consists of three primary hardware components: the power supply, thermoelectric module, and heatsinks. The refrigerator was manufactured within the mechanical workshop at Hamdard University. The structure was designed so as to ensure the insulation required and to fit the cooling elements. A compact portable solution was pursued, having the internal dimensions of 12 cm × 17 cm x 24 cm, resulting in a refrigeration capacity of 4.896 litres. The dimensional analysis of the fridge therefore yields a volume of 4896 cm^3, and a refrigeration area of 1800 cm^2, with a total power consumption of 108.6 W.

Relying on the computations and on the dimensional constraints of the components to be integrated, a 3D CAD model of the refrigeration system was designed in SolidWorks (Fig. 3).

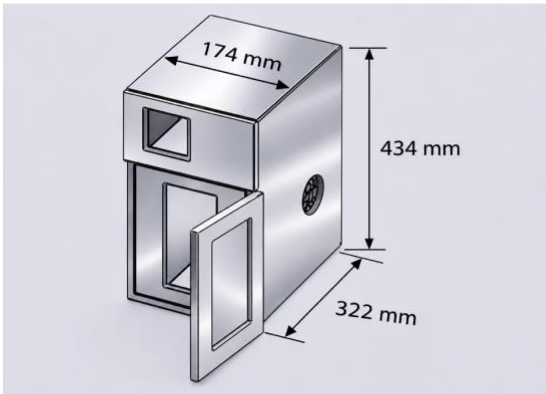

Fig. 3 – CAD model of the thermoelectric refrigerator casing.

3. EXPERIMENTAL TESTS

The experimental configuration for the portable thermoelectric refrigerator (Fig. 4) was established through a systematic procedure encompassing system sizing and design, component selection, manufacturing, and comprehensive thermal analysis [23]. The design commenced with the selection of a thermoelectric module, with an appropriate temperature difference specified and compatible with a 12 VDC power source.

The TEC1-12710 Peltier module [22] was selected due to its maximum operating current of 10.5 A, maximum voltage of 15.2 V, and maximum cooling capacity of 85 W at 25 °C hot-side temperature (96 W at 50 °C). The achievable temperature difference is 66 °C at 25 °C hot-side temperature, and 75 °C at 50 °C. The specifications make it suitable for the cooling requirements of the developed portable refrigerator. Throughout the experiments, the module was supplied from a 12 V / 20 A DC source, being powered at 12 V and ~6 A, thus operating below its rated power. The study, however, aims to compare the influence of different heatsinks and cooling loads under identical electrical operating conditions, with less focus on the thermoelectric module's performance.

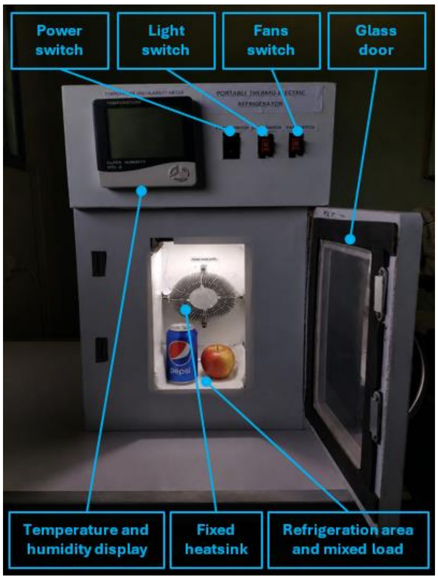

Fig. 4 – The portable thermoelectric refrigerator.

The heatsink selection and arrangement were essential for efficient thermal management. Four different heatsinks were used, one of them (Heatsink 4) being attached to the cold side (refrigeration area), while the other three heatsinks were used in turn on the hot side. A copper block and thermal grease were employed to improve thermal conductivity between the TEC module and the heatsinks. The system's performance was assessed by varying the cooling loads with several specimens and heatsink combinations under both natural and forced convection conditions.

Temperature measurements were performed to determine the required cooling range and the temperature difference imposed on the thermoelectric module. The cooling load was determined using the load mass, specific heat, and the desired cooling. A maximum average heat transfer rate of 114.83 W was calculated with relations (3) and (5), for a temperature decrease of 40.4 °C, over 120 minutes (from 30.4 °C to -10 °C, measured with a thermocouple).

4. TESTING CONDITIONS FOR THE THERMOELECTRIC REFRIGERATOR

The heat transfer rate and coefficient of performance were determined for each test case. The thermodynamic computations included the mass and specific heat capacity of each item, corroborated with constant temperature difference and the duration required to achieve thermal stability.

The properties of the refrigerated items used in the experiment are listed in Table 2. For combined specimens, the values represent the sum of individual specific heat capacities, used as a comparative thermal load indicator.

Table 2

Specimens and their combinations [24]

No.	Specimen	Mass m [kg]	Thermal capacity indicator Σc_p [J/kg·K]
1.	Beverage can	0.25	4180
2.	Apple	0.185	3640
3.	Potato	0.165	3390
4.	Beverage can and apple	0.435	7830
5.	Beverage can and potato	0.415	7580
6.	Apple and potato	0.35	7030
7.	Beverage can, apple and potato	0.6	11220

For all specimens and their combinations, the total heat removed was estimated, from which the heat transfer rate was derived. Subsequently, the COP_R was calculated as the ratio between the average cooling rate and the electrical input power. The refrigerator was tested under four conditions to evaluate the cooling load effect. To investigate the impact of combined cooling loads, we tested four combinations of specimens. The external temperature of the refrigerator was consistently maintained at 30 °C, under the same ambient and operational settings, employing Heatsink 1 with forced convection for all scenarios.

- **Condition 1: Beverage can and apple** to assess the cooling of both liquid and solid items simultaneously.
- **Condition 2: Beverage can and potato**, to investigate the influence of a solid specimen with different thermal properties, such as specific heat capacity, density and water content.
- **Condition 3: Apple and potato**, to observe the cooling load impact of two solid specimens with similar thermal behavior.
- **Condition 4: Beverage can, apple and potato**, combining all three specimens, as the maximum cooling load scenario.

5. RESULTS

5.1. EFFECT OF HEATSINK CONFIGURATION

The heat transfer rate and coefficient of performance were assessed for three hot side heatsinks, under natural and forced convection conditions. The tests were performed without a refrigerated specimen to determine the influence of the heatsink configuration solely.

As shown in Fig. 5, Heatsink 1 exhibited the highest heat transfer rate in both convection modes.

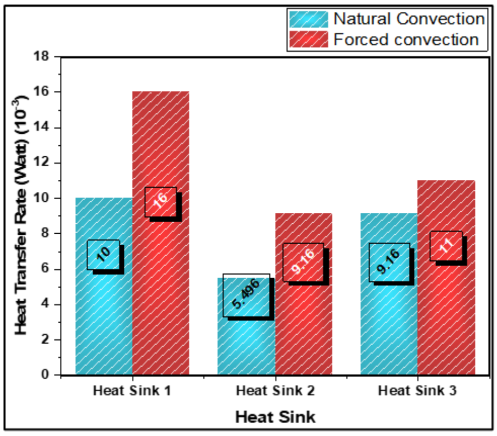

Fig. 5 – Heat transfer rates comparison of different heatsinks.

Heatsink 1's higher heat dissipation efficiency is attributed to its enhanced thermal conductivity and a larger surface area. Heatsink 2 showed the lowest heat transfer rate, indicating a limited capacity to remove heat effectively, likely due to its smaller surface area or less efficient fin geometry. Heatsink 3 showed intermediate performance. Forced convection increased the heat transfer rate for all three heatsinks compared with natural convection.

Similar trends were obtained for the coefficient of performance, presented in Fig. 6. Heatsink 1 achieved the highest COP under both natural and forced convection, Heatsink 2 had the lowest values, whereas Heatsink 3 exhibited intermediate performance.

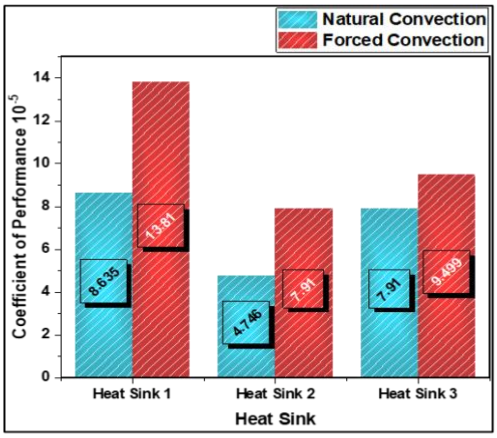

Fig. 6 – COP comparison of different heatsinks.

The results show that the performance of the portable thermoelectric refrigerator depends on both hot side heat dissipation, as well as on the cooled load properties. The best results were achieved with Heatsink 1 under forced convection conditions, outlining its superior thermal efficiency and effective heat dissipation capabilities. Henceforth, Heatsink 1 with forced convection was used for the subsequent tests with individual and combined cooling loads. These results underscore the importance of optimal heatsink design in enhancing the energy efficiency of thermoelectric refrigeration systems. The trends are in agreement with the literature, showing that improved heat dissipation enhances the cooling performance of thermoelectric refrigerators [1, 18, 21].

5.2. INDIVIDUAL COOLING LOADS

A comparison of the cooling time and coefficient of performance for different individual specimens, as well as with empty refrigerator, is presented in Fig. 7, under a constant temperature decrease of approximately 12 °C. Due to its liquid content, the beverage can requires the longest cooling time, liquids possessing a higher heat content and specific heat capacity, resulting in a slower cooling process.

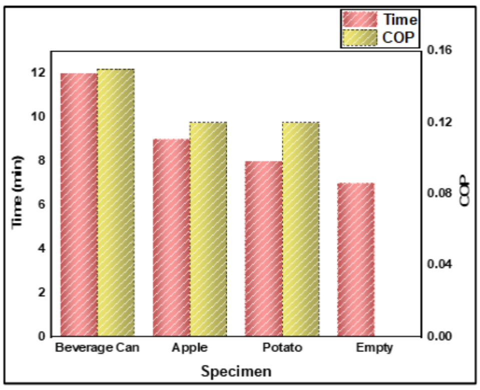

Fig. 7 – Cooling time and COP for individual cooling loads.

The empty refrigerator reaches the target temperature within the shortest time due to the absence of a significant thermal load. Regarding energy efficiency, the increase in COP is due to the increase in the average cooling rate.

The apple and potato exhibit similar values, consistent with their lower mass and thermal capacity. These results highlight the influence of individual material properties on cooling performance and system efficiency.

The experiments with individual items show that cooling time is influenced by the thermal characteristics of the refrigerated products. The longer cooling time of the beverage may be attributed to the thermal properties of liquids, generally having relatively high specific heat capacities, that require a larger amount of heat to be removed to achieve the same temperature reduction. Moreover, heat has to be transferred throughout a liquid volume, contributing to the slower transient cooling process. Product mass, specific heat capacity, geometry, exposed surface area and internal structure contribute to the process. As expected, the empty refrigerator reaches the target temperature the fastest, as the thermal load is only represented by the air volume inside.

5.3. COMBINED COOLING LOADS

Fig. 8 presents the cooling time and coefficient of performance for all the four combinations of specimens under a constant temperature difference of 12 °C. The results indicate that the refrigeration process depends not only on the number of refrigerated products, but also on their thermal characteristics. The beverage can–apple–potato combination required the longest cooling time due to the largest overall thermal load. This combination exhibited the highest average heat transfer rate and COP under the test conditions.

The results demonstrate that both the cooling time and the energy consumption are strongly dependent on the cumulative thermal load of the refrigerated contents.

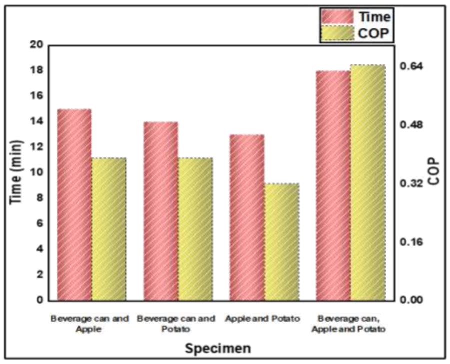

Fig. 8 – Cooling time and COP for combined cooling loads.

Figure 9 illustrates the heat transfer rates of all the specimens and combinations of specimens at a constant temperature difference of 12 °C. The results show the gradual increase in the heat transfer rate, from the empty refrigerator to the combined cooling loads, reaching a maximum value for the beverage can–apple–potato combination. This is expected, since larger cooling loads contain more thermal energy to be removed during the cooling process. Though the cooling time increases with the load size, the total heat extracted was also greater, resulting in higher heat transfer rates. This is mainly due to the beverage can, that has an important contribution owing to its liquid content, which stores more thermal energy than the solid items. Hence, the combinations with beverage can exhibit higher heat transfer rates than the apple–potato combination. This trend reflects the balance between increasing thermal load and extended cooling time, in agreement with the average cooling rate defined by eq. (5).

For the combined loads, the cooling time increased as additional specimens were introduced, with the combination of all three items requiring the longest period. At the same time, the average heat transfer rate and COP increased since the total amount of heat removed increased more than the cooling time. This indicates a greater quantity of heat removed per unit time.

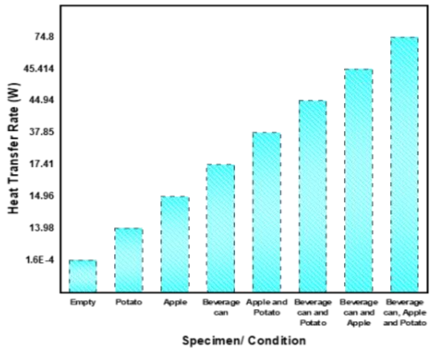

Fig. 9 – Heat transfer rate for individual and combined cooling loads.

6. CONCLUSIONS

The present study focuses on the performance of a portable thermoelectric refrigerator and experimentally demonstrates that the thermal characteristics of refrigerated products have a measurable influence on the cooling process.

The results indicate that the type, physical state, and combination of different thermal loads affect the cooling time, heat transfer rate, and coefficient of performance, highlighting the importance of evaluating thermoelectric refrigerators under realistic operating conditions rather than only with an empty compartment.

The experimental results further demonstrate that the overall performance of the refrigerator depends both on the effectiveness of hot-side heat dissipation and on the combined effect of the loads. Consequently, both the heatsink configuration and the thermal characteristics of the items to be refrigerated should be considered when optimizing portable thermoelectric refrigeration systems.

Future work will focus on the development of a coupled thermoelectrical numerical model to support predictive performance analysis and the optimization of thermoelectric refrigeration systems under different cooling loads and operating conditions.

ACKNOWLEDGEMENT

The authors would like to acknowledge the support of the technicians from the Mechanical Engineering Workshop, Faculty of Engineering Science and Technology, Hamdard University Karachi, Sindh, Pakistan.

CREDIT AUTHORSHIP CONTRIBUTION STATEMENT

GHULAM RAZA SHAH RIZVI: investigation, data curation, methodology, hardware.

RAHOOL RAI: formal analysis, conceptualization, writing (draft), validation, supervision, project administration.

CLAUDIA-IRINA SĂVESCU: conceptualization, writing (draft, review and editing), visualization, validation.

Received on May 14, 2026

REFERENCES

1. Z. Chen, M. Liao, X. Hu, Y. Ma, S. Jiang, X. Chen, F. Zou, X. Fan, Z. He, *Study on the performance of a thermoelectric refrigerator under natural convection heat transfer conditions*, Applied Thermal Engineering, **230**, p. 120822 (2023).
2. X. Lv, Y. Fu, Y. Mao, H. Gu, L. Wang, C. Dong, J. Shen, *Research on multi-space portable box based on thermoelectric refrigeration technology*, Applied Thermal Engineering, **263**, p. 125368 (2025).
3. E. A. Elibol, M. Z. Yilmazoglu, A. E. Aksoy, F. Aktas, *Thermal analysis of a refrigeration system integrated with a thermoelectric couple and microchannels using TiO2-water nanofluid*, International Journal of Heat and Fluid Flow, **108**, p. 109491 (2024).
4. V. Oruç, A. G. Devecioğlu, *Experimental assessment of the retrofit of an internal heat exchanger in refrigeration systems: The effect on energy performance and system operation*, Applied Thermal Engineering, **180**, p. 115843 (2020).
5. Y. N. Nandanwar, P. V. Walke, V. P. Kalbande, M. Mohan, *Performance improvement of vapour compression refrigeration system using phase change material and thermoelectric generator*, International Journal of Thermofluids, **18**, p. 100352 (2023).
6. Q. Xu, B. Deng, Y. Wang, W. Liu, G. Chen, *Small, affordable, ultra-low-temperature vapor-compression and thermoelectric hybrid freezer for clinical applications*, Cell Reports Physical Science, **4**, *12*, p. 101735 (2023).
7. C. Săvescu, A. M. Morega, M. Roman, C. Nechifor, *Experimentally validated studies of thermoelectric generators installed on a compressor test bench*, Rev. Roum. Sci. Techn. – Électrotechn. et Énerg., **70**, *2*, pp. 193–198 (2025).
8. Y. Qu, E. Pan, F. Zhu, F. Jin, A. K. Roy, *Modeling thermoelectric effects in piezoelectric semiconductors: New fully coupled mechanisms for mechanically manipulated heat flux and refrigeration*, International Journal of Engineering Science, **182**, p. 103775 (2023).
9. A. Morega, M. Morega, M. Panait, *Structural optimization of a thermoelectric generator by numerical simulation*, Rev. Roum. Sci. Techn. – Électrotechn. et Énerg., **55**, *1*, pp. 3–12 (2010).
10. C. Harsito, R. Delfianti, R. Syahroni, F. Nusyura, F. Minelli, *Effect of aspect ratio on thermoelectric system performance for waste heat recovery as alternative energy in building*, Results in Engineering, **26**, p. 105115 (2025).
11. A. Belkaid, I. Colak, K. Kayisli, *A direct adaptive sliding mode high voltage gain peak power tracker for thermoelectric applications*, Rev. Roum. Sci. Techn. – Électrotechn. et Énerg., **66**, *2*, pp. 131–136 (2021).
12. E. Rovianto, R. Delfianti, F. Minelli, C. Harsito, R. Podder, S. R. Joshua, *Crossflow Thermoelectric Kitchen Hood System for Enhancing Sustainable Energy in Buildings*, Civil Engineering Journal, **12**, *6*, pp. 2402–2414 (2026).
13. F. Săftoiu, A.-M. Morega, *Cooling system for photovoltaic panels*, Rev. Roum. Sci. Techn. – Électrotechn. et Énerg., **67**, *3*, pp. 343–348 (2022).
14. H. K. Badaka, A. M. Morega, *Simulation of biomass carbonization and heat recovery for electricity production using Seebeck modules*, Rev. Roum. Sci. Techn. – Électrotechn. et Énerg., **69**, *3*, pp. 353–358 (2024).
15. D. Dima, A. Dobrovicescu, C. Ioniță, C. Dobre, *Exergy analysis of the coupling of two CO2 heat pump cycles*, Rev. Roum. Sci. Techn. – Électrotechn. et Énerg., **68**, *2*, pp. 236–240 (2023).
16. Y. Hu, B. Shen, *Experimental insights into thermoelectric freezer systems: Feasibility and efficiency*, Energy Conversion and Management: X, **23**, p. 100676 (2024).
17. O. Kuznyetsov, V. V. Atamaniuk, *Energy-based model of a liquid piston gas compression system*, Rev. Roum. Sci. Techn. – Électrotechn. et Énerg., **70**, *1*, pp. 145–150 (2025).
18. F. Afshari, M. Akif Ceviz, E. Mandev, F. Yıldız, *Effect of heat exchanger base thickness and cooling fan on cooling performance of Air-To-Air thermoelectric refrigerator; experimental and numerical study*, Sustainable Energy Technologies and Assessments, **52**, p. 102178 (2022).
19. B. Abderezzak, R. K. Dreepaul, K. Busawon, D. Chabane, *Experimental characterization of a novel configuration of thermoelectric refrigerator with integrated finned heat pipes*, International Journal of Refrigeration, **131**, pp. 157–167 (2021).
20. A. P. M. Cüce, T. Güçlü, E. Cuce, *The Effect of Nanofluid Usage on Electricity Consumption in Thermoelectric Refrigeration Application: An Experimental Study*, GJES, **8**, *2*, pp. 228–236 (2022).
21. N. Alam, M. Salman Ali, S. Sajid, D. Sharma, Z. Hasan, *Experimental investigation and analysis of cooling performance of solar thermoelectric refrigerator*, Solar Energy, **263**, p. 111892 (2023).
22. *** *Thermoelectric Cooler TEC1-12710*, Hebei I.T. (Shanghai) Co., Ltd., https://www.hebeiltd.com.cn/peltier.datasheet/TEC1-12710.pdf.
23. E. Fenton, M. Bozorgi, S. Tasnim, S. Mahmud, *Solar-powered thermoelectric refrigeration with integrated phase change material: An experimental approach to food storage*, Journal of Energy Storage, **79**, p. 110247 (2024).
24. *** *Food and Foodstuff - Specific Heat*, The Engineering ToolBox (2003), https://www.engineeringtoolbox.com/specific-heat-capacity-food-d_295.html.